Ripple Wave Vector Rotation in Anisotropic Crystal Sputtering

S. Rusponi, G. Costantini, C. Boragno, and U. Valbusa

INFM–Unitá di Ricerca di Genova e Centro di Fisica delle Superfici e delle Basse Temperature del CNR, Dipartimento di Fisica dell'Universitá, Genova, Italy

(Received 11 June 1998)

Surface morphology of a Cu(110) crystal, generated by ion sputtering, has been investigated by scanning tunneling microscopy. Different from recent theoretical predictions and experimental results, normal sputtering produces a well defined ripple structure whose wave vector rotates from $\langle 001 \rangle$ to $\langle 1\bar{1}0 \rangle$ by increasing the substrate temperature. Off-normal sputtering at low temperature (180 K) generates ripples whose orientation depends on both ion direction and surface azimuthal orientation. These results are described by a continuum equation which includes both surface curvature dependent erosion terms and diffusion terms accounting for surface anisotropy and Ehrlich-Schwoebel barriers. [S0031-9007(98)07159-2]

PACS numbers: 68.35.Bs, 61.16.Ch

Understanding of the formation of peculiar morphologies during ion sputtering has received increasing interest in the past years. Experimental studies on amorphous materials [1,2] and semiconductor amorphized by ion bombardment [3–5] show that off-normal ion sputtering at room temperature generates a modulation of the surface (ripples). Depending on the ion incidence angle θ, the ripple wave vector can be either perpendicular (θ close to grazing) or parallel (θ close to normal) to the component of the ion beam in the surface plane, while for normal incidence ($\theta \cong 0°$) no periodic structures are present. These results have been theoretically explained in terms of a linear instability caused by the surface curvature dependent sputtering, which competes and dominates the smoothing due to the thermal surface diffusion [6,7]. On the contrary, in quite similar experimental conditions, ion sputtering on single crystal metals produces features that reflect the substrate symmetry without any relationship with the ion beam direction: Square pits have been observed on Cu(001) [8] and Ag(001) [9]; hexagonal ones on Pt(111) [10], Au(111) [11], and Cu(111) [12]; and ripples with crests oriented along $\langle 1\bar{1}0 \rangle$ on Ag(110) [13]. A recent paper [14] has shown that ripple structures similar to those observed on amorphous materials can also be produced by sputtering on Cu(110) at low temperature (180 K), showing that the surface evolution results from competition between diffusion, limited at the step edges by a Schwoebel barrier, and erosion.

In this Letter we intend to clarify the characteristics of this competition aiming to describe in a unified framework the origin of the various morphologies observed on metals. We propose to modify the continuum equation proposed by Cuerno and Barabasi for amorphous substrates [7] (in the following, referred to as the CB model), including a term that takes into account the effect of a Schwoebel barrier on diffusion [15,16]. This model is able to explain all of the features previously observed on other metal surfaces as well as new experimental results obtained by sputtering Cu(110) for different values of surface temperature T_S, ion beam direction θ, and azimuthal angle δ [see Fig. 1(a)]. The experimental data show two relevant results: (1) independently on δ, normal sputtering ($\theta \cong 0°$) induces a ripple structure which rotates by 90° by increasing T_S; (2) off-normal ion sputtering produces ripples whose orientation depends on both θ and δ.

The experimental setup has been described elsewhere [13,17]. The Cu(110) crystal has been sputtered by 1 keV Ar^+ ions, for different values of the ion flux Φ and ion fluence Ψ, at temperature T_S and subsequently frozen at $T \approx 100$ K. Afterwards, surface morphology has been observed with an ultrahigh vacuum scanning tunneling microscope. In Fig. 1 we show the results obtained for $\theta = 0°$, $\delta = 0°$, and different T_S. At the lowest temperature considered ($T_S = 180$ K), the surface is rough [Fig. 1(b)]. For T_S in the range 250–270 K the surface morphology is characterized by a well defined ripple structure (wavelength $\cong 20$ nm) with the crests aligned along $\langle 001 \rangle$ [Fig. 1(c)]. A little increase in the sputtering temperature ($T_S = 320$ K) produces a degradation of this structure [Fig. 1(d)]. If T_S is further increased in the range 350–360 K, a second ripple structure (wavelength $\cong 100$ nm) appears [Fig. 1(e)], with the crests along $\langle 1\bar{1}0 \rangle$ (90° ripple rotation). Finally, at higher temperatures a quasi-layer-by-layer erosion is observed [Fig. 1(f)]. Similar results have also been reported on Ag(110) [13]. A wave vector dependence on the substrate crystallographic directions is also observed for off-normal ion incidence. In Fig. 2 we report the surface topography of Cu(110) after low temperature ($T_S = 180$ K) ion sputtering at $\theta = 45°$ and $\theta = 70°$ for different values of δ. Independent of δ, for θ close to grazing incidence ($\theta = 70°$), the morphology is characterized by a well defined ripple structure with the wave vector k perpendicular to the ion beam direction [Figs. 2(b), 2(d), 2(f)], similar to what is observed on amorphous substrates. On the contrary, ion sputtering at $\theta = 45°$ produces ripples with the wave vector parallel to $\langle 1\bar{1}0 \rangle$ for all values of δ

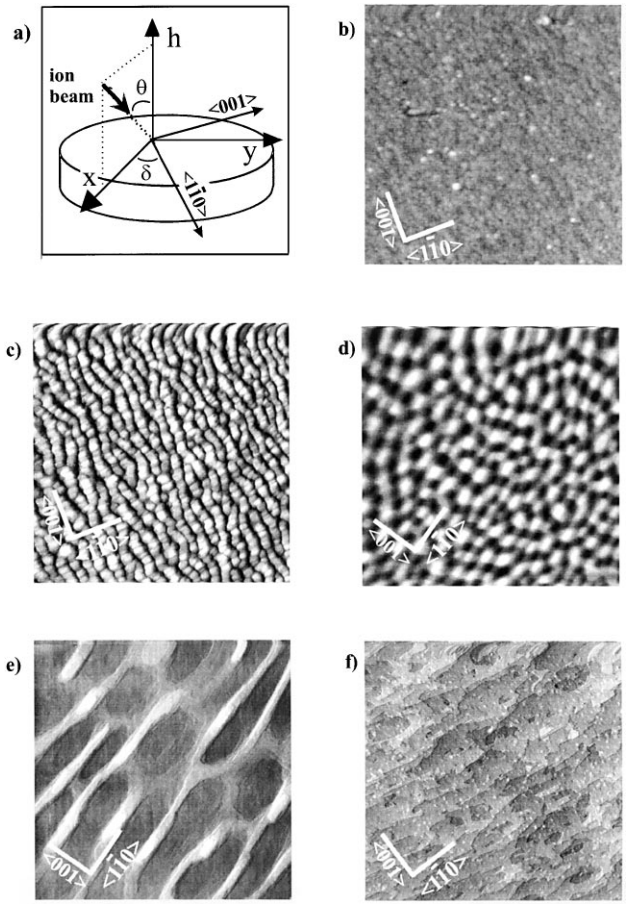

FIG. 1. Five images [size 400×400 nm^2 for (b) and (c), while for (d), (e), and (f) size is 800×800 nm^2] of Cu(110) after ion sputtering at normal incidence ($\theta = 0°$) for different temperatures T_S: 180 K (b), 250 K (c), 320 K (d), 360 K (e), and 400 K (f). $\Phi = 0.09$ ML/s, $\Psi = 80$ ML, and $\delta = 0°$. The inset (a) shows the experimental geometry, (x, y, h) represents the laboratory frame, h is the normal to the flat surface, while ion trajectories are assumed to lie in the x-h plane.

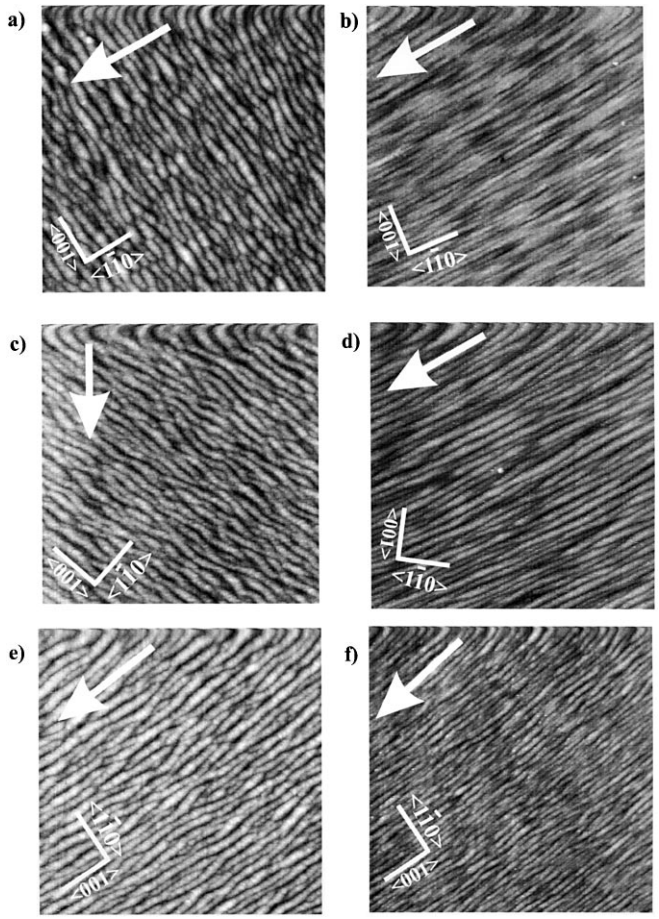

FIG. 2. Six images (size 400×400 nm^2) after ion sputtering at $T_S = 180$ K for $\theta = 45°$ (a),(c),(e) and $\theta = 70°$ (b),(d),(f). The value of the azimuthal angle is $\delta = 0°$ in (a) and (b), $\delta = 45°$ in (c) and (d), and $\delta = 90°$ in (e) and (f). The white arrow indicates the ion beam direction.

considered [Figs. 2(a), 2(c), 2(e)]. This last result is completely different from that reported on amorphous materials and amorphized semiconductors for which off-normal ion sputtering with $\theta \leq \theta_c$ ($\theta_c \cong 60°$ [6,7]) produces ripples with wave vectors always parallel to the ion beam.

In a previous paper [14], the study of the scaling laws characterizing the time and spatial evolution of the ripples in the low temperature regime suggested that the presence of a Schwoebel barrier, limiting the interlayer mass transport, could lead to a surface instability overcoming the one due to ion erosion. A similar explanation was recently proposed by Murty *et al.* [11] to account for pit coarsening in sputtered Au(111). To explain the present data and, more generally, the morphology of all of the metal sputtered surfaces, we suggest modifying the diffusive term $-D\nabla^2(\nabla^2 h)$ in the CB model. In fact, this term describes only an isotropic diffusion on a flat surface and does not take into account that the adatom (or vacancy) mobility on a single crystal metal surface is actually biased both in the vertical direction, by a Schwoebel barrier at the step edges, and in the surface plane, by a diffusion rate which, for (110), is different along the two crystallographic directions. For Cu(110) and in the simple case of $\delta = 0°$ ($\langle 1\bar{1}0 \rangle$ parallel to the x axis [Fig. 1(a)]) the diffusion term has the following form:

$$-S_{001}\frac{\partial^2 h}{\partial y^2} - S_{1\bar{1}0}\frac{\partial^2 h}{\partial x^2} - D_{001}\frac{\partial^4 h}{\partial y^4} - D_{1\bar{1}0}\frac{\partial^4 h}{\partial x^4}, \quad (1)$$

where all of the coefficients are positive. $S_{001} \propto 1 - R_{001}$ and $S_{1\bar{1}0} \propto 1 - R_{1\bar{1}0}$ [16], where $R_{001} = e^{-E_{S_{001}}/kT}$ and $R_{1\bar{1}0} = e^{-E_{S_{1\bar{1}0}}/kT}$ are the ratio of the probability to hop to a lower layer versus the probability to bound back on the terrace; $D_{001} \propto e^{-E_{D_{001}}/kT}$ and $D_{1\bar{1}0} \propto e^{-E_{D_{1\bar{1}0}}/kT}$ [6,18] where $E_{D_{001}}$ and $E_{D_{1\bar{1}0}}$ represent the energy barriers for surface diffusion, respectively, along $\langle 001 \rangle$ and $\langle 1\bar{1}0 \rangle$. Since in Cu(110) the activation energy for vacancy diffusion is higher than the one for adatoms [19], as already discussed in Ref. [14], we limit ourselves to consider

only the adatom mobility. In this case $E_{S_{001}} = 0.27$ eV, $E_{S_{1\bar{1}0}} = 0.19$ eV, $E_{D_{001}} = 0.42$ eV, and $E_{D_{1\bar{1}0}} = 0.29$ eV [19]. Following Ref. [20] we have assumed a constant prefactor for all of the atomistic processes $\cong 10^{12}$ s^{-1}. The first two terms in (1) account for the asymmetry in the interlayer diffusion generated by the presence of a Schwoebel barrier at the step edges [21–23] while the last two describe the diffusion on a flat surface [18,24,25].

With this change, the equation for time evolution of h [7] during *normal sputtering* ($\theta = 0°$) becomes

$$\frac{\partial h}{\partial t} = -\nu_0 + \gamma \frac{\partial h}{\partial x} + (\nu_x - S_{1\bar{1}0}) \frac{\partial^2 h}{\partial x^2} + (\nu_y - S_{001}) \frac{\partial^2 h}{\partial y^2} + |A(E,\theta)|\nabla^2 h + \frac{\lambda_x}{2}\left(\frac{\partial h}{\partial x}\right)^2 + \frac{\lambda_y}{2}\left(\frac{\partial h}{\partial y}\right)^2 - D_{1\bar{1}0} \frac{\partial^4 h}{\partial x^4} - D_{001} \frac{\partial^4 h}{\partial y^2} + \eta . \quad (2)$$

The term $|A(E,\theta)|\nabla^2 h$ has been suggested by Carter and Vishnyakov [26] to account for the smoothing effect due to the recoiling adatom diffusion induced by irradiation at a given energy E, while the coefficients γ, ν, and λ depend on ion flux, θ, and deposited energy distribution [see Eq. (5) of Ref. [7]]. Similar to what is discussed in Ref. [7], a Laplacian term with a negative coefficient leads to a ripplelike instability, in the time evolution of h, characterized by a wave vector k oriented along the direction (x or y) for which the absolute value of the coefficient of the Laplacian term is the largest one. As a consequence, when Eq. (2) holds, the surface morphology will be determined by a competition among the two roughening terms $\nu_x - S_{1\bar{1}0}$, $\nu_y - S_{001}$ and the smoothing one $|A(E,\theta)|$. Since the S coefficients, contrary to ν and A, are temperature dependent, T_S determines which term dominates among the three. At the lowest temperature ($T_S = 180$ K) $D_{1\bar{1}0}/D_{001} \cong 4 \times 10^3$, implying that adatom diffusion is activated only along $\langle 1\bar{1}0\rangle$, and as a consequence D_{001} and S_{001} have a negligible effect. Thus, the previous three terms become $\nu_x - S_{1\bar{1}0}$, ν_y, and $|A(E,\theta)|$. Experimental data for sputtering at this temperature show a nonperiodic surface [Fig. 1(b)] characterized by a low value ($\approx$4 atomic layers) [14] of the roughness W (defined as the rms of the local height h [27]). Both of these results indicate a predominance of the smoothing term. For $T_S = 250$ K the diffusion rate along $\langle 1\bar{1}0\rangle$ increases ($-D_{1\bar{1}0}\partial^4 h/\partial x^4$ term) and thus, with respect to the $T_S = 180$ K case, the number of adatoms that try to diffuse to a lower layer is multiplied by a factor $D_{1\bar{1}0}(T_S = 250)/D_{1\bar{1}0}(T_S = 180) \cong 200$. However, when $R_{1\bar{1}0} \cong 10^{-4}$, the adatom thermal energy is not large enough to allow interlayer diffusion. Adatoms that reach a step edge rebound back on the terrace producing an uphill current some order of magnitude bigger than the one that occurs at $T_S = 180$ K ($-S_{1\bar{1}0}\partial^2 h/\partial x^2$). In the continuum equation this effect is represented by the predominance of $\nu_x - S_{1\bar{1}0}$ on the temperature independent terms A and ν_y, generating a surface instability with k parallel to the x direction [Fig. 1(c)]. At higher temperatures ($300 \le T_S \le 320$ K) $D_{1\bar{1}0}/D_{001} \cong 200$; as a consequence adatoms also begin to diffuse along $\langle 001\rangle$ and, being $E_{S_{1\bar{1}0}} + E_{D_{1\bar{1}0}} \cong E_{D_{001}}$ [19], overcome the Schwoebel barrier for the interlayer motion along $\langle 1\bar{1}0\rangle$. As a consequence the instability due to $-S_{001}\partial^2 h/\partial y^2$ starts to take on effectiveness to the detriment of that due to $-S_{1\bar{1}0}\partial^2 h/\partial x^2$. Thus both x and y instabilities are present and the surface is characterized by rectangular mounds randomly arranged [Fig. 1(d)]. For sputtering at $T_S = 350$ K, only interlayer motion in the $\langle 001\rangle$ direction is inhibited [$R_{001} \cong (5 \times 10^{-2}) R_{1\bar{1}0}$], and the surface shows a ripple structure with k along the y direction [Fig. 1(e)]. Finally if $T_S \ge 380$ K, adatoms can also overcome the second step edge barrier and the smoothing effect due to the fourth-order terms in (2) prevails [Fig. 1(f)].

For *off-normal sputtering* ($\theta \neq 0°$) at $T_S = 180$ K (see Fig. 2) we can neglect $|A(E,\theta)|\nabla^2 h$ ($|A(E,\theta)|$ decreases rapidly to zero with increasing θ [26]), D_{001}, and S_{001} (since at low temperature diffusion is prevalently activated along $\langle 1\bar{1}0\rangle$). Thus we can write (2), in the case of $\delta = 0°$ (i.e., $\langle 1\bar{1}0\rangle$ parallel to the x axis), as

$$\frac{\partial h}{\partial t} = -\nu_0 + \gamma \frac{\partial h}{\partial x} + (\nu_x - S_{1\bar{1}0}) \frac{\partial^2 h}{\partial x^2} + \nu_y \frac{\partial^2 h}{\partial y^2} + \frac{\lambda_x}{2}\left(\frac{\partial h}{\partial x}\right)^2 + \frac{\lambda_y}{2}\left(\frac{\partial h}{\partial y}\right)^2 - D_{1\bar{1}0} \frac{\partial^4 h}{\partial x^4} + \eta . \quad (3)$$

Surface morphology will now be determined by the competition between $\nu_x - S_{1\bar{1}0}$ and ν_y. For $\theta = 45°$, being $\nu_x < \nu_y < 0$ [7], k is parallel to the x direction [Fig. 2(a)]. On the other hand, for $\theta = 70°$, $\nu_y < 0 < \nu_x$ [7] and, since k turns out to be parallel to the y direction [Fig. 2(b)], we can infer that $\nu_y < \nu_x - S_{1\bar{1}0}$.

Completely different results are obtained for $\delta = 90°$ ($\langle 001\rangle$ aligned along x axis) when (3) becomes

$$\frac{\partial h}{\partial t} = -\nu_0 + \gamma \frac{\partial h}{\partial x} + (\nu_y - S_{1\bar{1}0}) \frac{\partial^2 h}{\partial y^2} + \nu_x \frac{\partial^2 h}{\partial x^2} + \frac{\lambda_x}{2}\left(\frac{\partial h}{\partial x}\right)^2 + \frac{\lambda_y}{2}\left(\frac{\partial h}{\partial y}\right)^2 - D_{1\bar{1}0} \frac{\partial^4 h}{\partial y^4} + \eta . \quad (4)$$

Now the surface morphology is related to the competition between the $\nu_y - S_{1\bar{1}0}$ and ν_x coefficients. For $\theta = 70°$, being $\nu_y - S_{1\bar{1}0} < 0 < \nu_x$, k is parallel to the y direction similar to the $\delta = 0°$ case. On the contrary, a new effect can be observed for $\theta = 45°$. In fact, although $\nu_x < \nu_y < 0$, if $S_{1\bar{1}0}$ is large enough, $|\nu_y - S_{1\bar{1}0}|$ can be larger than $|\nu_x|$, leading to a ripple structure with k again parallel

to the y direction. If this is the case no ripple rotation is expected, as we have experimentally observed [Figs. 2(e) and 2(f)]. More complex is the discussion for $0° < \delta < 90°$ which will be reported elsewhere together with an extensive study of the scaling laws [28]. However, independent of the value of δ, from Fig. 2 we can deduce that for $\theta = 45°$ surface morphology is dominated by the instability due to surface diffusion, biased by a Schwoebel barrier [Eq. (1)], while at grazing angles it is determined by erosion.

The model presented has a general validity for (110) surfaces in the presence of a Schwoebel barrier for adatoms (or vacancies) and is able to explain all of the morphologies observed after ion sputtering. In the case of (111) or (100) surfaces, as those described in Refs. [8–12], Eq. (1) has to be modified in order to account for the different symmetry directions and energy diffusion barriers [28].

In conclusion, we have shown that on a single crystal metal the surface morphology produced by ion sputtering depends on both ion erosion and surface diffusion processes. We have also proposed an equation to explain the experimental results. The equation is a modified version of the one proposed by Cuerno and Barabasi for amorphous materials [7] in which we have included a diffusive term that accounts both for the presence of a Schwoebel barrier at the step edges and for the anisotropic surface diffusion.

[1] M. Navez, C. Sella, and D. Chaperot, Compt. Rend. **254**, 240 (1962).
[2] T. M. Mayer, E. Chason, and A. J. Howard, J. Appl. Phys. **76**, 1633 (1994).
[3] G. W. Lewis, M. J. Nobes, G. Carter, and J. L. Whitton, Nucl. Instrum. Methods **170**, 363 (1980).
[4] E. Chason, T. M. Mayer, B. K. Kellerman, D. T. McIlroy, and A. J. Howard, Phys. Rev. Lett. **72**, 3040 (1994).
[5] J. J. Vajo, R. E. Doty, and E. Cirlin, J. Vac. Sci. Technol. A **14**, 2709 (1996).
[6] R. M. Bradley and J. M. E. Harper, J. Vac. Sci. Technol. A **6**, 2390 (1988).
[7] R. Cuerno and A. L. Barabasi, Phys. Rev. Lett. **74**, 4746 (1995).
[8] M. Ritter, M. Stindtmann, M. Farle, and K. Baberschke, Surf. Sci. **348**, 243 (1996).
[9] G. Costantini, S. Rusponi, C. Boragno, and U. Valbusa, Surf. Sci. (to be published).
[10] T. Michely and G. Comsa, Nucl. Instrum. Methods Phys. Res., Sect. B **82**, 207 (1993).
[11] R. M. V. Murty, T. Curcic, A. Judy, and B. H. Cooper, Phys. Rev. Lett. **80**, 4713 (1998).
[12] J. Naumann, J. Osing, A. J. Quinn, and I. V. Shvets, Surf. Sci. **388**, 212 (1997).
[13] S. Rusponi, C. Boragno, and U. Valbusa, Phys. Rev. Lett. **78**, 2795 (1997).
[14] S. Rusponi, G. Costantini, C. Boragno, and U. Valbusa (to be published).
[15] R. L. Schwoebel, J. Appl. Phys. **40**, 614 (1969).
[16] G. Ehrlich and H. Hudda, J. Chem. Phys. **44**, 1039 (1966).
[17] R. Conti, S. Rusponi, D. Pagnotta, C. Boragno, and U. Valbusa, Vacuum **48**, 639 (1997).
[18] M. A. Makeev and A. L. Barabasi, Appl. Phys. Lett. **71**, 2800 (1997).
[19] P. Stolze, J. Phys. Condens. Matter **6**, 9495 (1994).
[20] C. L. Liu, J. M. Cohen, J. B. Adams, and A. F. Voter, Surf. Sci. **253**, 334 (1991).
[21] M. D. Johnson, C. Orme, A. W. Hunt, D. Graff, J. Sudijomo, L. M. Sander, and B. G. Orr, Phys. Rev. Lett. **72**, 116 (1994).
[22] J. Krug, M. Plischke, and M. Siegert, Phys. Rev. Lett. **70**, 3271 (1993).
[23] M. Siegert and M. Plischke, Phys. Rev. Lett. **73**, 1517 (1994).
[24] C. Herring, J. Appl. Phys. **21**, 301 (1950).
[25] Z. W. Lai and S. DasSarma, Phys. Rev. Lett. **66**, 2348 (1991).
[26] G. Carter and V. Vishnyakov, Phys. Rev. B **54**, 17 647 (1996).
[27] A. L. Barabasi and H. E. Stanley, *Fractal Concepts in Surface Growth* (Cambridge University Press, Cambridge, England, 1995).
[28] S. Rusponi, G. Costantini, C. Boragno, and U. Valbusa (to be published).